Research Square

Preprints are preliminary reports that have not undergone peer review.
They should not be considered conclusive, used to inform clinical practice,
or referenced by the media as validated information.

# Research on the Structural Features and Regulatory Effect of Polysaccharides in Ganoderma lucidum on TAMs

**Juan Du**

dujuan@zzwzy.edu.cn

ZhangzhouHealth Vocational College

**Ze Dang**

Jiamusi University

**Chuanli Jin**

Jiamusi University

**Yu Fu**

Jiamusi University

**Ruian Ma**

Jiamusi University

**Chen Chen**

Jiamusi University

**Qinglin Bian**

Jiamusi University

**Peng Lv**

ZhangzhouHealth Vocational College

**Yanhu Ji**

ZhangzhouHealth Vocational College

**Weicheng Gao**

ZhangzhouHealth Vocational College

**Shunhui Liu**

ZhangzhouHealth Vocational College

**Research Article**

**Keywords:** G. lucidum, polysaccharide, TAMs

**Posted Date:** May 25th, 2026

**DOI:** https://doi.org/10.21203/rs.3.rs-9497793/v1

**License:** This work is licensed under a Creative Commons Attribution 4.0 International License.
Read Full License

**Additional Declarations:** No competing interests reported.

# Abstract

This experiment purified GLAP-2 from Ganoderma lucidum through Sepharose 6B and Sephacryl S-300 HR gradient elution, collected it by freeze-drying, and obtained GLAP-2 with a uniform molecular weight of $3.7\times10^4$ Da. Its total polysaccharide content was 79.79%, and the content of galacturonic acid was 23.82%. GLAP-2 was free of protein.

Infrared spectroscopy analysis indicated that GLAP-2 had characteristic absorption peaks. The results of monosaccharide composition analysis showed that GLAP-2 was composed of 1,6-Glc *p* residues and 1,3-Glc *p* residues alternately linked, with a *β*-glucan structure. Structure characterization revealed that GLAP-2 possessed a backbone composed of 1→4-linked *β*-D-Glcp, or an alternating 1→4-linked main chain of *β*-D-Glcp and *α*-D-Glcp; *α*-D-Manp and *β*-D-GlcpA are attached to the main chain as side-chain residues.

The immune activity assay showed that GLAP-2 did not inhibit the growth of RAW264.7 cells, but could promote the secretion of TNF-α, NO, and IL-6 by IL-4-induced TAMs. The expression levels of TNF-α, NO, and IL-6 in M2 macrophages were significantly lower than those in M0 macrophages, and the expression levels of TNF-α, NO, and IL-6 significantly increased with the increase of GLAP-2 concentration. This indicates that our study successfully induced M2 and M1 macrophages in RAW264.7 cells using GLAP-2, and GLAP-2 can significantly inhibit the polarization of M2 macrophages and promote their transformation into M1 macrophages.


# 1. Introduction

The innate immune system is the earliest barrier formed by the body against foreign pathogens and transformed tumor cells. Among them, macrophages, as the first line of defense of the human immune system, serve as an important cellular bridge connecting innate immunity and acquired immunity[1]. Macrophages are heterogeneous and plastic, and can respond to different environments from resting state (M0) polarization to different activation states[2]. In TME, its function responds to the activation of microenvironmental signals and is polarized into two phenotypes, namely the classical activation pathway M1 type and the alternate activation pathway M2 type[3]. M1 type is called classically activated macrophages, which mainly exist in the proinflammatory environment and are induced by inflammatory mediators such as lipopolysaccharide, IFN-γ, TNF-*α* and GM-CSF. M2 type through a different pathway from M1, e.g., it can be activated by cytokines (IL-4, IL-13), vitamin D3, transforming growth TGF-*β*, PGE2 and glucocorticoids. The main function of M2 is to limit the immune response by secreting inhibitory cytokines IL-10 and TGF-*β*[4], promote tumor invasion, growth and metastasis, and prevent T cells from playing an effective anti-tumor role. In TME, most of TAMs exist in the form of M2 macrophages[5], which can directly promote the proliferation and activation of tumor cells[6], and exert immunosuppressive effects through many ways in the tumor microenvironment. Therefore, the research on natural polysaccharides targeting TAMs and reversing their mediated immunosuppressive function has attracted extensive attention in the scientific community.

Polysaccharides are representative biomolecules that play an extremely important role in nature. In recent decades, numerous bioactive polysaccharide-protein complexes and polysaccharides have been extracted from plants, lichens, algae, yeasts, fungi, and mushrooms, garnering significant attention for their anti-tumor and immune-regulating properties[7]. Among them, natural polysaccharide is a potential natural antitumor drug because of its safety and unique immunomodulatory properties. Current studies have shown that several polysaccharides can transform immunosuppressed TAMs into M1 phenotype and significantly impede tumor progression. Notable examples include polysaccharides derived from *Moringa oleifera* leaf, *Cordyceps militaris*, yeast, *Dendrobium officinale*, and *Cistanche deserticola*[8–12]. Polysaccharides belong to pathogen-associated molecular patterns that activate immune responses by recognizing receptors. Receptors that have been shown to recognize polysaccharides include mannose receptors, scavenger receptors, Toll-like receptors (TLRs), DC-associated C-type lectin 1 (Dectin-1), and complement receptor 3 (CR3).

For a very long time, Chinese medicine has employed *Ganoderma lucidum* (Leyss. ex Fr.) Karst. to cure and prevent a wide range of human ailments. In the second century B.C., Shen Nong's Materia Medica listed *G. lucidum* as a medication of "high grade," meaning a herb with medical efficacy and no toxicity. Famous ancient Chinese physician Li Shi-Zhen also documented the effectiveness and medicinal use of *G. lucidum* in the 16th-century Ben Cao Gang Mu, the world-famous Compendium of Materia. One of the main tenets of traditional Chinese medicine, "*Fuzheng Guben*," or strengthening body resistance and consolidating the constitution of patients, was believed to be possible with *G. lucidum*, according to ancient Chinese medical academics[13]. In recent decades, the study of bioactive substances such as polysaccharides, triterpenoids, sterols, proteins and peptides in the fruiting body of *G. lucidum* has been the focus of biological and pharmacological research related to *G. lucidum*. Polysaccharides, an important active substance in Ganoderma, have been widely studied and reported in recent decades. Among them, the immunomodulatory activity of Ganoderma polysaccharides has been widely recognized, e.g., *G. lucidum* polysaccharides can alter the activity of numerous immune system constituents, including dendritic cells, T and B lymphocytes, NK cells, neutrophil granulocytes, and antigen-presenting cells[14–19].The stimulation of *G. lucidum* spore polysaccharide (GLSP) has been shown to induce overexpression of TNF-$\alpha$, IL-1$\beta$, IL-6, and TGF-$\beta$, as well as the polarization of primary macrophages towards the M1 phenotype. Additionally, GLSP promotes the release of various inflammatory agents and cytokines, thereby altering the composition of the tumor microenvironment[20].

Based on this, in this study, we extracted, isolated and purified the polysaccharide of *G. lucidum*, screened out the active homogeneous polysaccharide, and characterized its structure to explore its mechanism of mediating TAMs and reversing the phenotype of macrophages in the tumor microenvironment to activate the immune effect. This is very important for the research and development of *G. lucidum* related drugs and the establishment of quality control methods.

## 2. Materials and methods

## 2.1. Materials

*G. lucidum* was picked in July 2022 in Yunnan Province, China and identified by Professor Juan Du as the dried fruiting body of *G. lucidum* plants of polyporaceae. Toyopearl DEAE-650 M was purchased from TOSOH Co. (Tokyo, Japan). Sepharose 6B and Sephacryl S-300 HR were obtained from GE Healthcare (Amersham Biosciences AB, Uppsala, Sweden). Monosaccharide standards (L-Arabinose, L-Ara; D-Xylose, D-Xyl; L-Rhamnose, L-Rha; L-Fucose, L-Fuc; D-Mannose, D-Man; D-Glucose, D-Glc; D-Galactose, D-Gal; galacturonic acid, D-GalA; glucuronic acid, GlcA), Methyl iodide, TFA, DMSO, Sodium borodeuteride, Chloroform, Phenol, and 1-phenyl-3-methyl-5-pyrazolone (PMP) were purchased from Sigma (St. Louis, MO, USA) and domestic companies. Acetic anhydride were purchased from Mettlter-Toledo companies. Methanol were purchased from Panasonic Co., Ltd. Acetonitrile were purchased from Thermo Fisher Co., Ltd. Ammonium acetate were purchased from Shanghai Aladdin Biochemical Technology Co., Ltd. Sodium hydroxide were purchased from Sinopharm Chemical Reagent Co., Ltd. Concentrated sulfuric acid, Acetic acid, ethanol and Sodium Chloride were purchased from Tianjin Benchmark Chemical Reagent Co., Ltd. m-Hydroxydiphenyl was purchased from Beijing Dingguo Changsheng Biotech Co., Ltd.

## 2.2. Extraction, isolation and purification of polysaccharides

The *G. lucidum* polysaccharide was extracted using the water extraction and alcohol precipitation method. 1.5 kg *G. lucidum* were dried at 50 ℃, cut into small pieces and extracted with 95% ethanol for 24 h to remove impurities and small lipophilic molecules. The degreased powders were dried, and extracted three times by hot water reflux, 2 h each time. After filtration through defatted cotton, concentration in vacuo, and centrifugation was employed at 5500 rpm for 10 min to remove the residues. The supernatant was concentrated and precipitated with 80% EtOH (final concentration) at 4 ℃ overnight. The upper alcohol solution was concentrated and recovered. The precipitated sugar solution was redissolved with water, centrifuged at 5500 rpm, and the upper supernatant was dialyzed in a dialysis bag with a molecular weight of 3.5 kDa in pure water for 72 h. The water was changed every 6 h. The dialysate was lyophilized to obtain a crude polysaccharide fraction of GLCP (17.7 g, 1.18%).

Ion exchange and gel permeation chromatography were used for the separation of GLCP. Firstly, weigh 0.6 g of GLCP, dissolve it in 90 mL of pure water, stir well, and centrifuge (5500 rpm, 10 min) to obtain the supernatant. The supernatant was loaded on a Toyopearl DEAE 650M column (5.0 i.d.× 30 cm), which were successively eluted with $H_2O$; 0.2, 0.4, 0.6, 0.8 and 1.0 M NaCl solution. The fraction eluted with $H_2O$ was named GLN, and the fraction eluted with 0.2 M NaCl was named GLA. The fractions eluted with 1.0 and 2.0 M NaCl contained scarcely any polysaccharide. In addition, the major fraction of GLA was eluted through gradient elution procedure with 0.05, 0.1, 0.15, and 0.2 M NaCl to give two fractions: GLA-1 and GLA-2 (Fig. 1A). GLN was chromatographed by gel permeation on a Sepharose 6 B column (5.0 cm × 100 cm) and eluted with 0.1 M NaCl to obtain a major fraction. This major fraction was further purified on a Sephacryl S-300 HR column (2.2 cm × 100 cm) to yield purified polysaccharides, which were named GLNP (1348 mg) (Fig. 1A). GLA-1 was chromatographed by gel permeation on a Sepharose 6 B column (5.0 cm × 100 cm) and eluted with 0.1 M NaCl to obtain a major fraction. This major fraction was further purified on a Sephacryl S-300 HR column (2.2 cm × 100 cm) to yield purified polysaccharides, which

were named GLAP-1 (307 mg) (Fig. 1A). GLN was chromatographed by gel permeation on a Sepharose 6 B column (5.0 cm × 100 cm) and eluted with 0.1 M NaCl to obtain a major fraction which were named GLAP-2 (612 mg) (Fig. 1A).

## *2.3. Evaluation of fundamental physicochemical properties, purity, and homogeneity*

The phenol-$H_2SO_4$ method and the m-hydro-xydiphenyl method[21], were used to determine the amounts of total carbohydrates and uronic acid, respectively. As standards, galacturonic acid and galactose were utilized. Using BSA as the standard, a Bio-Rad protein assay kit was used to determine the protein concentration.Chemical composition (%, w/w), and sugar composition (Area %) purified polysaccharide from *Ganoderma lucidum* in Table 1.

Weigh out 5 mg of Prulan series (molecular weights of 6.1, 9.6, 21.1, 47.1, 107, 194, 337 and 642 kDa) polysaccharide standard, dissolve it in 5 mL of pure water, and prepare a 1 mg/mL Prulan series standard solution. Then, prepare a 0.02 mol/L $CH_3COONH_4$ solution as the mobile phase. Take 5 mL of the Prulan series standard solution and add it to the HPLC vial. Perform HPGPC analysis. Plot the standard curve using the retention time A on the vertical axis and the logarithm of molecular weight C on the horizontal axis.

Take 5 mg of the polysaccharide sample and dissolve it in 5 mL of pure water to prepare the sample solution. Wash the polysaccharide sample with $CH_3COONH_4$ solution as the mobile phase and perform HPGPC analysis. Determine the uniformity of the polysaccharide sample by their retention time and calculate its molecular weight.

## 2.4. Analysis of monosaccharide composition

Preparation of pure polysaccharide samples: 1 mg of the polysaccharide sample was weighed and dissolved in 1 mL of pure water. TFA (4 mol/L) was then added and the mixture was heated in a metal reaction bath. The sample was vacuum-dried to remove excess TFA until no acid taste was detected. The hydrolyzed polysaccharide sample was dissolved in pure water, mixed with NaOH solution, and transferred to a hydrolysis tube. PMP methanol solution was then added, and the mixture was vortex-shaken and incubated at 30 ℃ for 30 min. The mixture was cooled to room temperature, HCl was added to neutralize it, and then an equal volume of chloroform was added for extraction. The lower chloroform layer was discarded, and the mixture was transferred to a liquid chromatography vial.

Preparation of standard solution: Precision weighed 9 types of monosaccharides (Man, Rha, GlcA, GalA, Glc, Gal, Xyl, Ara, and Fuc) at 1 mg each, and mixed them together before dissolving them in 9 mL of pure water to prepare a 1 mg/mL mixed standard solution. Precision 1 mL of the mixed standard solution was then drawn and added to NaOH solution, which was transferred to a hydrolysis tube. PMP methanol solution was added, mixed, and incubated at 30°C for 30 min. HCl was added to neutralize the mixture, and the remaining steps were the same as those described above.

PMP monosaccharide chromatography conditions: Column: Diamonsil $C_{18}$ (250×4.6 mm); detection wavelength: 235 nm; injection volume: 7 μL; column temperature: 40 ℃. Flow rate of A (ammonium acetate buffer solution): 0.8 mL/min, flow rate of B (acetonitrile): 0.2 mL/min, total flow rate: 1 mL/min, gradient elution for 60 min.

## 2.5. FT-IR analysis

The FT-IR spectrum was obtained using a Fourier transform infrared spectrophotometer (Nicolet 5700, Thermo Co. Ltd., USA) within the range of 4000 – 400 $cm^{-1}$. The sample was ground with spectroscopic grade potassium bromide (KBr) powder and pressed into 1 mm pellets for FT-IR measurements.

## 2.6. Methylation analysis

Add 5 mg of the polysaccharide sample to 1 mL of DMSO and stir until completely dissolved. Then, grind NaOH quickly into a fine powder. Take 20 mg of the fine powder and add it to the sample, stirring for 1 hour. Place the sample in ice and add 250 μL of iodomethane, followed by pure water in ice to stop the reaction. Transfer the sample reaction mixture to a hydrolysis tube and dry with $N_2$ until the solution turns from turbid to clear. Extract with an equal volume of chloroform, followed by extraction with pure water, and dry with $N_2$. Add 4 mol/L TFA solution to the hydrolysis tube for heating hydrolysis, then cool down to room temperature. Next, add ammonia solution and $NaDB_4$ powder, followed by acetic acid solution to stop the reaction. After drying with $N_2$ gas flow, add acetic anhydride and 1-methylimidazole. Finally, add water at room temperature to stop the reaction. Extract the reaction liquid using chloroform and collect and combine the chloroform layer for transfer into a small gas phase bottle for GC-MS analysis.

The GC-MS injection conditions are as follows: helium carrier gas at a split ratio of 40:1; detector temperature at 240 ℃; column temperature ranging from 80 ℃ to190 ℃. Determine the mass spectrum form based on retention time on mass spectrometry graph for each sample compound, and calculate their content ratios in terms of fragment molecular weight.

## 2.7. NMR spectroscopy

$^{1}H$ NMR and $^{13}C$ NMR spectra of the purified polysaccharide were recorded in an NMR apparatus. 30 mg of the purified polysaccharide was dissolved in deuterium oxide, and was then dried at a vacuum freeze drier.

## 2.8 Immunosuppressive Effect of Ganoderma lucidum Homopolysaccharide on Tumor-Associated Macrophages (TAMs)

## 2.8.1 Determination of RAW264.7 Cell Viability Induced by GLAP-2

Mouse macrophage RAW264.7 cells were cultured in Dulbecco's Modified Eagle Medium (DMEM) supplemented with 10% fetal bovine serum (FBS) and maintained in a 37 °C incubator with 5% carbon dioxide ($CO_2$) for static culture.RAW264.7 cells in the logarithmic growth phase were seeded into 96-well plates at a density of $1\times10^5$ cells per well. After cell adherence, GLAP-2 was added to the 96-well plates at final concentrations of 500, 200, 100, and 50 μg/mL, followed by co-cultivation for 24 h. Subsequently, 10 μL of 3-(4,5-dimethylthiazol-2-yl)-2,5-diphenyltetrazolium bromide (MTT) reagent was added to each well and incubated for 4 h.A triplet reagent (composed of 10% sodium dodecyl sulfate, 5% isobutanol, and 0.012 mol/L hydrochloric acid (HCl), dissolved in distilled water) was added to dissolve the purple formazan crystals for 4–6 h. The absorbance at 570 nm ($OD_{570}$) was measured, and cell viability was calculated accordingly.

### 2.8.2 Determination of Cytokine Expression During Polarization of M0 and M2 Macrophages to M1 Phenotype

RAW264.7 cells and TAMs were separately cultured at a density of $5\times10^5$ cells/mL for 24 h, then stimulated with GLAP-2 at different concentrations (50, 100, and 200 μg/mL) for another 24 h before analysis.The expressions of interleukin-10 (IL-10), tumor necrosis factor-α (TNF-α), and interleukin-6 (IL-6) in macrophages were detected using enzyme-linked immunosorbent assay (ELISA) kits and Griess kits. After 24 h of incubation, the cell culture medium from each group was collected.A total of 100 μL of standard solution or GLAP-2 sample was added to each well, followed by 50 μL of enzyme-labeled antibody working solution. The plate was washed four times and then incubated at room temperature for 180 min. Subsequently, 100 μL of chromogenic reagent was added to each well, and the plate was incubated at room temperature for 20–25 min in the dark. After adding 100 μL of stop solution to each well and mixing thoroughly, the absorbance at 450 nm ($OD_{450}$) was measured immediately after calibration.

## 3. Results and discussion

## 3.1. Preparation and physicochemical properties of GLCP and purified polysaccharides

*G. lucidum* was extracted with hot water, precipitated with ethanol, dialyzed, and lyophilized, and then weighed to obtain 17.7 g of crude Ganoderma lucidum polysaccharides, with a yield of 1.18%. It was named GLCP.

Water-soluble GLCP was extracted from the dried powder of *G. lucidum* by hot water extraction, ethanol precipitation, dialysis, and lyophilization. The total extract yield was 1.18% (*w*/*w*). Each purified polysaccharide was obtained by separating the crude fraction of GLCP through combined ion-exchange column chromatography on DEAE-650 M and gel filtration chromatography on Sepharose 6B and Sephacryl S-300 HR. As a result, a neutral polysaccharide, GLNP, were finally obtained from GLN. Two acidic polysaccharides, GLAP-1 and GLAP-2, were finally obtained from GLA-1. The yields are shown in

the experimental section. The contents of total sugar, protein and uronic acid were determined by colorimetric analysis, as shown in Table 1 Additionally, each sample exhibited a single and symmetrical peak on the corresponding HPGPC chromatogram, as observed in Fig. 1B, suggesting good homogeneity in the molecular weight distribution.

Table 1
Chemical composition (%, w/w), and sugar composition (Area %) purified polysaccharide from *Ganoderma lucidum*

| **Chemical composition(%)** | **GLAP-1** | **GLAP-2** |
|---|---|---|
| **Total carbohydrate a** | **80.72** | **79.79** |
| **Uronic acid b** | **7.53** | **23.82** |
| **Protein c** | **1.14** | **2.08** |
| Monosaccharide composition (Area %) | | |
| Man | 3.6 | 1.6 |
| Rha | - | - |
| GlcA | 3.8 | 10.1 |
| GalA | - | - |
| Glc | 87.1 | 88.3 |
| Gal | 5.5 | - |
| Xyl | - | - |
| Ara | - | - |
| Fuc | - | - |
| a: Determined by phenol–H2SO4 method; | | |
| b: Determined by m-hydroxydiphenyl method; | | |
| c: Determined by Bio-Rad protein assay kit | | |

# 3.2. Structural characterization of GLAP-2

Methylation analysis is widely used to characterize the linkage patterns of sugar units in polysaccharides. By comparing with the CCRC spectral database, the GC-MS spectra of partially methylated alditol acetates of GLAP-2 are shown in Table 2 and Fig. 2.

Among them, GLAP-2 contains 2-mannopyranose residues (2-Manp), which is consistent with previous literature reports. GLAP-2 is mainly composed of t-glucopyranose residues, 2,3,4-glucopyranose residues, 3-glucopyranose residues, 4-glucopyranose residues and 3,4-glucopyranose residues. It is inferred that the main chain linkage consists of 1,6-glucopyranose residues and 1,3-glucopyranose residues[22].In addition, the content of *α*-D-glucopyranose residues (*α*-D-Glc*p*-(1→)) in GLAP-2 is relatively high, which may be related to its relatively low molecular weight. Meanwhile, it may also be attributed to the short length of their main chains, resulting in a short rod-like or spherical conformation.

Table 2
Methylation analysis results of polysaccharides GLAP-2

| **Peaks** | **$t_R$ (min)** | **Sugar derivatives** | **GLAP-2** |
|---|---|---|---|
| 1 | 15.441 | 2-Man*p* | 4.63% |
| 2 | 17.643 | t-Glc*p* | 42.80% |
| 3 | 19.995 | 3-Glc*p* | 11.16% |
| 4 | 20.258 | 4-Glc*p* | 8.74% |
| 5 | 20.702 | 2,3,4-Glc*p* | 22.56% |
| 6 | 23.016 | 3,4-Glc*p* | 10.12% |

# 3.3 NMR spectroscopy analysis

The ¹H NMR signals of GLAP-2 are mainly concentrated in the range of 0.5–5.4 ppm, and the

¹³C NMR signals are mainly concentrated in the range of 55.0–110.0 ppm, indicating that GLAP-2 has characteristic absorption peaks of polysaccharides. GLAP-2 appears to have multiple terminal hydrogen signals in the range of 4.5–5.4 ppm and multiple anomeric carbon signals in the range of 95.0–110.0 ppm, which indicates the presence of multiple sugar residues in it. According to the downfield chemical shifte of the pyranose residues, if the anomeric proton signal is δH > 5.0, it indicates α-configuration. Conversely, if the anomeric proton signal is δH < 5.0, it indicates *β*-configuration[23]. In Fig. 3A, the presence of strong peaks at δH 5.15 ppm and δH 5.06 ppm indicates that GLAP-2 contains α-type sugar residues, while the signal at δH 4.47 ppm suggests the presence of β-type sugar residues in GLAP-2, which is consistent with the analysis results of FT-IR. As shown in Fig. 3B, the appearance of signals in the high field region of δ 170–180 ppm indicates that GLAP-2 contains acidic sugar residues, further confirming it is an acidic polysaccharide. Through further comprehensive analysis of the one-dimensional and two-dimensional nuclear magnetic resonance spectra of GLAP-2 and review of relevant literatures, the chemical shifts of residues in GLAP-2 were summarized (Table 2). For residue A, cross signals of C-1 to C-6 were identified in the HSQC spectrum at δ 4.45/103.0, δ 3.33/73.0, δ 3.67/75.5, δ

3.66/81.03, δ 3.58/75.9, and δ 3.84/60.7. Among these, the signals of C-3 (δC 75.5) and C-6 (δC 60.7) shifted to the low field due to the conjugation effect. Combined with the analysis by Säwén E[24], Residue A was inferred to be →4)-*β*-D-Glcp-(1→. Using the same method, the H1/C1 to H6/C6 signals of Residue B were determined: the cross signals of Residue B are as follows: δ 5.15/91.8, δ 3.45/71.5, δ 3.87/73.4, δ 3.54/75.4, δ 3.85/69.9, and δ 3.66/60.6. This determination was made by combining the monosaccharide composition of GLAP-2 and relevant literature[25].The glycosidic linkage of Residue B was inferred to be →4)-*α*-D-Glcp-(1→. For the remaining sugar residues, the chemical shifts of H-2/C-2 to H-6/C-6 were assigned in a similar manner. Through analysis of relevant literature[26], Residue C was identified as α-D-Man*p*-(1→, which is consistent with the results of methylation analysis. Residue D exhibited a typical anomeric carbon signal of *β*-glucuronic acid[27], The most critical characteristic is that the chemical shift of C6 was δ 174.9 ppm; due to the presence of the carboxyl group (-COOH), this signal was shifted upfield by approximately 110 ppm compared with the C6 of ordinary glucose, which serves as a sample basis for glucuronic acid[28].Residue D was identified as *β*-D-Glc*p*A-(1→ This identification was supported by relevant literature[29]. As shown in Fig. 3C, the H2 of sugar Residue A exhibited long-range coupling with its own C3. This indicates that the C2-H and C3 of Residue A are separated by 2–3 bonds (consistent with spatial/electronic transmission within the pyranose ring), further confirming that Residue A is a pyranose residue. Similarly, the H2 of sugar Residue B showed long-range coupling with its own C5, supporting that Residue B is α-D-glucopyranose. The C4 chemical shift of Residue A (δ 81.03 ppm) was downfield-shifted by approximately 6–11 ppm compared with that of free glucose C4 (67.0–75 ppm), directly confirming that Residue A has a 1→4 glycosidic linkage. The C4 chemical shift of Residue B (δ 75.4 ppm) was downfield-shifted by approximately 5–10 ppm relative to free glucose C4, proving that Residue B also has a 1→4 glycosidic linkage. In the HMBC spectrum, a B(H2)-D(C1) correlation signal was observed: the H2 of Residue B (δ 3.45 ppm) showed long-range coupling with the anomeric carbon (C1) of Residue D (δ 102.5 ppm). Additionally, an HMBC correlation existed between the signal of H-3 in Residue C (δ 3.81 ppm) and the signal of C-5 in Residue B (δ 69.9 ppm), confirming long-range coupling between the H3 proton of Residue C and the C5 carbon nucleus of Residue B.

In summary, GLAP-2 is composed of →4)-*β*-D-Glc*p*-(1→, →4)-*α*-D-Glc*p*-(1→, α-D-Manp-(1→, and *β*-D-GlcpA-(1→. Given that →4)-*β*-D-Glcp-(1→ has the highest content, it is inferred that GLAP-2 has either a main chain consisting of 1→4-linked *β*-D-Glc*p*, or an alternating 1→4-linked main chain of *β*-D-Glc*p* and α-D-Glc*p*; α-D-Manp and *β*-D-Glc*p*A are attached to the main chain as side-chain residues.The $^{1}H$ and $^{13}C$ NMR chemical shifts of GLAP-2 are listed in Table 3.

Table 3

**$^{1}$H NMR and $^{13}$C NMR Chemical shifts of GLAP-2.**

| Polysaccharide | Glycosyl residues | Chemical shifts $\delta$(ppm) | | | | | |
|---|---|---|---|---|---|---|---|
| | | H1 | H2 | H3 | H4 | H5 | H6 |
| | | C1 | C2 | C3 | C4 | C5 | C6 |
| GLAP-2 | A: →4)-β-D-Glcp-(1→ | 4.45 | 3.33 | 3.67 | 3.66 | 3.58 | 3.84 |
| | | 103.0 | 73.0 | 75.5 | 81.03 | 75.9 | 60.7 |
| | B: →4)-α-D-Glcp-(1→ | 5.15 | 3.45 | 3.87 | 3.54 | 3.85 | 3.66 |
| | | 91.8 | 71.5 | 73.4 | 75.4 | 69.9 | 60.6 |
| | C: α-D-Manp-(1→ | 5.06 | 4.07 | 3.81 | 3.69 | 3.93 | 3.81/3.91 |
| | | 101.2 | 70.4 | 71.4 | 67.1 | 73.1 | 60.9 |
| | D: β-D-GlcpA-(1→ | 4.48 | 3.39 | 3.55 | 3.45 | 3.65 | 174.9 |
| | | 102.5 | 75.23 | 78.06 | 74.15 | 80.57 | |

(D) Effects of GLAP-2 on NO secretion by macrophages and TAMs;(E) Effects of GLAP-2 on IL-10 secretion by macrophages and TAMs

RAW264.7 cells were treated with GLAP-2 at different concentrations (50, 100, 200, and 500 μg/mL) for 48 hours, and the MTT assay was used to detect cell viability. As shown in Fig. 4A, when RAW264.7 cells were treated with GLAP-2 at concentrations ranging from 50 to 500 μg/mL, it was confirmed that GLAP-2 had no inhibitory effect on the viability of RAW264.7 cells. The results indicated that GLAP-2 exhibited no significant toxicity to RAW264.7 cells within the concentration range of 50, 100, 200, and 500 μg/mL.

## 3.4 *Determination of Cytokine Expression during Polarization of M0- and M2-Type Macrophages to M1-Type Macrophages*

As shown in Fig. 4BCD, in the determination of nitric oxide (NO) content, 100 μg/mL GLAP-2 significantly increased the NO production in RAW264.7 macrophages ($p < 0.01$) and elevated the concentration of NO secreted by macrophages, which is crucial for resisting pathogens or foreign substances. Subsequently, we determined its effect on the production of tumor necrosis factor-α (TNF-α), interleukin-10 (IL-10), NO, and interleukin-6 (IL-6) in RAW264.7 cells. Compared with the untreated control group, within the concentration range of 50, 100, and 200 μg/mL, GLAP-2 significantly increased the TNF-α production in RAW264.7 cells ($p < 0.001$). Within the concentration range of 100 and 200 μg/mL, GLAP-2 significantly enhanced the IL-6 production in RAW264.7 cells ($p < 0.001$). Among them, TNF-α and IL-6 are major pro-inflammatory cytokines, and the release of TNF-α and IL-6 can stimulate the innate immune response. Therefore, the intervention of GLAP-2 promoted the production of TNF-α, NO, and IL-6, and induced the

unpolarized RAW264.7 cells to acquire the M1 phenotype. Within the concentration range of 50 and 100 μg/mL, GLAP-2 significantly increased the IL-10 production in RAW264.7 cells ($p < 0.01$, $p < 0.001$).

Compared with the untreated control group, 100 μg/mL GLAP-2 also promoted the NO expression in IL-4-induced tumor-associated macrophages (TAMs) ($p < 0.01$). Within the concentration range of 50, 100, and 200 μg/mL, with the increase of GLAP-2 concentration, the IL-6 production in IL-4-induced TAMs was significantly increased ($p < 0.05$, $p < 0.01$, $p < 0.001$). Within the concentration range of 50, 100, and 200 μg/mL, GLAP-2 significantly upregulated the TNF-α expression in IL-4-induced TAMs ($p < 0.001$). The expression levels of TNF-α, NO, and IL-6 in IL-4-induced TAMs treated with GLAP-2 were significantly lower than those in RAW264.7 cells treated with GLAP-2. These results indicated that M2-type and M1-type macrophages were successfully induced from RAW264.7 cells in this study, and GLAP-2 could significantly inhibit the polarization of M2-type macrophages and promote their conversion to M1-type.

## 3.5 Discussion

The biological activity of polysaccharides is affected by their molecular size, degree of branching, and conformation. For instance, a larger molecular weight of β-glucan is associated with more significant antitumor effects[30]. In this experiment, the molecular weight of GLAP-2 was $3.7\times10^4$ Da, which was higher than that of the heteropolysaccharide LZ-D-1 obtained by Ye et al[31]. It is thus inferred that GLAP-2 may exhibit more prominent immunomodulatory activity. Additionally, the ratio of 1,3-Glc*p* to 1,6-Glc*p* in GLAP-2 is approximately 1:1, suggesting that its main chain structure might differ from the alternately linked 1,3-Glcp and 1,6-Glcp pattern reported in previous literatures.

It is known that *β*-glucans with the same chemical structure from *Ganoderma lucidum* exist in a rigid chain conformation (resembling ordered trimers) in aqueous solutions, and undergo conformational transition in alkaline solutions[32]. This indicates that under the same chemical structure, changes in conformation or molecular weight can lead to different biological activities of polysaccharides, confirming the close correlation between polysaccharide structure and biological activity.

In the tumor microenvironment (TME), macrophages account for 50% of the infiltrating leukocytes. In vitro, macrophages can exert antitumor effects by producing cytotoxic molecules such as TNF-α, IL-12, and NO. However, tumor-associated macrophages (TAMs) mostly promote tumor growth rather than inhibit it. Mantovani et al[33], proposed that TAMs may differentiate into alternatively activated M2-type macrophages upon exposure to IL-4 and IL-10. These M2-type macrophages exhibit enhanced phagocytic activity and increased expression of mannose/galactose receptors, while showing impaired expression of reactive nitrogen intermediates. They produce ornithine and polyamines via the dehydrogenase pathway, express IL-1 decoy receptors, and display a phenotype of low IL-12 and high IL-10. This is consistent with the results of this study: when GLAP-2 acted on IL-4-induced TAMs, the levels of TNF-α, IL-12, and NO were lower than those when GLAP-2 acted directly on RAW264.7 cells. Therefore, screening effective agents such as bioactive natural products to selectively promote the polarization of TAMs towards the M1 type represents a promising therapeutic strategy for malignant tumors.

Studies have shown that glucans can convert immunosuppressive M2-like TAMs into M1-type macrophages, significantly delaying tumor progression[34]. The GLAP-2 isolated in this experiment has a glucan configuration and can promote the secretion of TNF-α, NO, and IL-6 by IL-4-induced TAMs. Since the expression levels of TNF-α, NO, and IL-6 in M2-type macrophages are significantly lower than those in M0-type macrophages, and the expression levels of these three molecules increased significantly with the increase in GLAP-2 concentration, it is confirmed that the glucan configuration of GLAP-2 can act on TAMs and induce their polarization towards the M1 type.

Furthermore, GLAP-2 can also promote the secretion of IL-10 by IL-4-induced TAMs, and the possible reasons include: (1) The TME is generally characterized by immunosuppression. As an immunosuppressive cytokine, IL-10 can inhibit excessive immune responses, and its production may increase accordingly[35]; (2) M1-type TAMs may release IL-10 together with other immunoregulatory factors such as PGE2 and TGF-β, synergistically promoting immunosuppression and tumor progression[36]; (3) TAMs may produce IL-10 as part of a feedback regulatory mechanism for inflammatory responses[37]. In conclusion, GLAP-2 can not only promote the activation of immune cells and enhance immune responses to combat infections and diseases, but also inhibit excessive immune responses, reduce inflammation and immune damage, which is beneficial for maintaining immune homeostasis and alleviating immune-related diseases.

# 4. Conclusion

In this study, homogeneous polysaccharides GLAP-1 and GLAP-2 were isolated from Ganoderma lucidum, and they had similar molecular weights. Among them, GLAP-2 was selected for subsequent structural characterization, and the results showed that there were differences in the monosaccharide compositions between the two polysaccharides. The biological activity of polysaccharides is affected by their molecular size, degree of branching, and conformation. The larger the molecular weight of *β*-glucan, the more significant its anti-tumor effect[38]. In this experiment, the molecular weight of GLAP-2 was $3.7\times10^4$ Da, which was higher than the heteropolysaccharide LZ-D-1[39]. According to this literature, GLAP-2 may have a more significant immune regulation effect. The same chemically structured *β*-glucan in *G. lucidum* exists in a rigid chain conformation in aqueous solution, similar to an ordered trimer, and undergoes conformation transformation in alkaline solution. Through the combined analysis of monosaccharide composition and methylation NMR data, it is inferred that GLAP-2 has either a main chain consisting of 1→4-linked *β*-D-Glcp, or an alternating 1→4-linked main chain of *β*-D-Glcp and α-D-Glcp; α-D-Manp and *β*-D-GlcpA are attached to the main chain as side-chain residues. In vitro experiments have confirmed that the homogeneous polysaccharide GLAP-2 from Ganoderma lucidum is non-toxic to RAW264.7 cells. GLAP-2 can not only induce M0-phenotype RAW264.7 cells to secrete TNF-α, NO, and IL-6, but also promote M2-phenotype tumor-associated macrophages (TAMs) induced by IL-4 to secrete TNF-α, NO, and IL-6. Moreover, with the increase of GLAP-2 concentration, the expression levels of TNF-α, NO, and IL-6 increase significantly. These results indicate that in this study, RAW264.7 cells were successfully induced into M2-type and M1-type macrophages. It was also confirmed that

GLAP-2 can regulate the expression of RAW264.7 cells into M1 phenotype in the tumor microenvironment (TME) and adjust the levels of various cytokines, thereby inhibiting tumor growth. Additionally, GLAP-2 can mediate TAMs, reverse the macrophage phenotype to activate immune effect mechanisms, and increase the level of IL-10 to resist excessive immune responses and cytokine storms.

## Declarations

# Fundings

High-level Talent Scientific Research Start-up Fund of Zhangzhou Health Vocational College under Grant No. BSKYQD-9.

# Author Contribution

Author contributionsJ.D. conceived and designed the study, supervised the research, and revised the manuscript.Z.D. and C.L.J. performed the polysaccharide purification, structural characterization (HPGPC, FT-IR, NMR, methylation analysis), and cell experiments (RAW264.7/TAM polarization assays).Y.F. and R.A.M. analyzed the experimental data and prepared the figures.C.C. and Q.L.B. contributed to the literature review and interpretation of the results.P.L., Y.H.J., and W.C.G. and S.H.L.provided technical support and reagents.All authors read and approved the final version of the manuscript.

# Acknowledgement

This work was supported by the High-level Talent Scientific Research Start-up Fund of Zhangzhou Health Vocational College under Grant No. BSKYQD-9.

## References

1. Nie C, Zhu P, Ma S, Wang M, Hu Y. Purification, characterization and immunomodulatory activity of polysaccharides from stem lettuce. Carbohydr Polym. 2018, 188:236–242. doi: 10.1016/j.carbpol.
2. Mantovani A, Allavena P, Sica A, Balkwill F. Cancer-related inflammation. Nature. 2008, 454(7203):436 – 44. doi: 10.1038/nature07205.
3. Gordon S, Martinez FO. Alternative activation of macrophages: mechanism and functions. Immunity. 2010, 32(5):593–604. doi: 10.1016/j.immuni.2010.05.007.
4. Ferreira SS, Passos CP, Madureira P, Vilanova M, Coimbra MA. Structure-function relationships of immunostimulatory polysaccharides: A review. Carbohydr Polym. 2015, 132:378 – 96. doi: 10.1016/j.carbpol.2015.05.079.

5. Komohara Y, Fujiwara Y, Ohnishi K, et al. Tumor-associated macrophages: Potential therapeutic targets for anti-cancer therapy. Adv Drug Deliv Rev, 2016, 99: 180–185. doi: 10.1016/j.addr.2015.11.009.
6. Komohara Y, Horlad H, Ohnishi K, et al. Importance of direct macrophage-Tumor cell interaction on progression of human glioma. Cancer Sci, 2012, 103(12): 2165–2172. doi: 10.1111/cas.12015.
7. Xie G, Schepetkin IA, Quinn MT. Immunomodulatory activity of acidic polysaccharides isolated from Tanacetum vulgare L. Int Immunopharmacol. 2007, 7(13):1639–1650. doi: 10.1016/j.intimp.2007.08.013.
8. Wang, S., Hu, Q., Chang, Z., Liu, Y., Gao, Y., Luo, X., Zhou, L., Chen, Y., Cui, Y., Wang, Z., Wang, B., Huang, Y., Liu, Y., Liu, R., Zhang, L. Moringa oleifera leaf polysaccharides exert anti-lung cancer effects upon targeting TLR4 to reverse the tumor-associated macrophage phenotype and promote T-cell infiltration. Food & function, 14(10) (2023) 4607–4620. doi: 10.1039/d2fo03685a.
9. Bi S, Huang W, Chen S, Huang C, Li C, Guo Z, Yang J, Zhu J, Song L, Yu R. Cordyceps militaris polysaccharide converts immunosuppressive macrophages into M1-like phenotype and activates T lymphocytes by inhibiting the PD-L1/PD-1 axis between TAMs and T lymphocytes. Int J Biol Macromol. 2020, 150: 261–280. doi: 10.1016/j.ijbiomac.
10. S.H. Albeituni, C.L. Ding, M. Liu, X.L. Hu, F.L. Luo, G. Kloecker, M. Bousamra 2nd, H.G. Zhang, J. Yan, Correction: yeast-derived particulate β-glucan treatment subverts the suppression of myeloid-derived suppressor cells (MDSC) by inducing polymorphonuclear MDSC apoptosis and monocytic MDSC differentiation to APC in cancer, J. Immunol. 196 (9) (2016) 3967, https://doi.org/10.4049/jimmunol.1600346.
11. Wang HY, Ge JC, Zhang FY, Zha XQ, Liu J, Li QM, Luo JP. Dendrobium officinale polysaccharide promotes M1 polarization of TAMs to inhibit tumor growth by targeting TLR2. Carbohydr Polym. 2022, 292:119683. doi: 10.1016/j.carbpol.2022.119683.
12. Jiang S, Cui Y, Wang B, Fu Z, Dong C. Acidic polysaccharides from Cistanche deserticola and their effects on the polarization of tumor-associated macrophages. Int J Biol Macromol. 2024, 282(Pt 4):137207. doi: 10.1016/j.ijbiomac.2024.137207.
13. Lin Z. Ganoderma (Lingzhi) in Traditional Chinese Medicine and Chinese Culture. Adv Exp Med Biol. 2019;1181:1–13. doi: 10.1007/978-981-13-9867-4_1.
14. Boh B, Berovic M, Zhang J, Zhi-Bin L. Ganoderma lucidum and its pharmaceutically active compounds. Biotechnol Annu Rev. 2007, 13:265–301. doi: 10.1016/S1387-2656(07)13010-6.
15. Wasser SP. Medicinal mushrooms as a source of antitumor and immunomodulating polysaccharides. Appl Microbiol Biotechnol. 2002, 60(3):258–274. doi: 10.1007/s00253-002-1076-7.
16. Chien CM, Cheng JL, Chang WT, Tien MH, Tsao CM, Chang YH, Chang HY, Hsieh JF, Wong CH, Chen ST. Polysaccharides of Ganoderma lucidum alter cell immunophenotypic expression and enhance CD56 + NK-cell cytotoxicity in cord blood. Bioorg Med Chem. 2004, 12(21):5603-9. doi: 10.1016/j.bmc.2004.08.004.

17. Hsu MJ, Lee SS, Lee ST, Lin WW. Signaling mechanisms of enhanced neutrophil phagocytosis and chemotaxis by the polysaccharide purified from Ganoderma lucidum. Br J Pharmacol. 2003, 139(2):289 – 98. doi: 10.1038/sj.bjp.0705243.
18. Cao LZ, Lin ZB. Regulation on maturation and function of dendritic cells by Ganoderma lucidum polysaccharides. Immunol Lett. 2002, 83(3):163-9. doi: 10.1016/s0165-2478(02)00087-1.
19. Lin YL, Liang YC, Lee SS, Chiang BL. Polysaccharide purified from Ganoderma lucidum induced activation and maturation of human monocyte-derived dendritic cells by the NF-kappaB and p38 mitogen-activated protein kinase pathways. J Leukoc Biol. 2005, 78(2):533 – 43. doi: 10.1189/jlb.0804481.
20. Song M, Li ZH, Gu HS, Tang RY, Zhang R, Zhu YL, Liu JL, Zhang JJ, Wang LY. Ganoderma lucidum Spore Polysaccharide Inhibits the Growth of Hepatocellular Carcinoma Cells by Altering Macrophage Polarity and Induction of Apoptosis. J Immunol Res. 2021 2021:6696606. doi: 10.1155/2021/6696606.
21. GustavAsboe-Hansen, N. B. (1973). New method for quantitative determination of uranic acids. Analytical Biochemistry, 54, 484–489.
22. Liu, W., Wang, H., Pang, X., Yao, W., & Gao, X.. Characterization and antioxidant activity of two low-molecular-weight polysaccharides purified from the fruiting bodies of Ganoderma lucidum. International journal of biological macromolecules, 2010, 46(4), 451–457. https://doi.org/10.1016/j.ijbiomac.2010.02.006
23. Zhang M, Liao J, Zhang Z, Shi H, Wu J, Huang W, Li C, Song L, Yu R, Zhu J. Structural characterization of two novel heteropolysaccharides from Catharanthus roseus and the evaluation of their immunological activities. Carbohydr Polym. 2025, 348(Pt B):122896. doi: 10.1016/j.carbpol.2024.122896.
24. Säwén E, Huttunen E, Zhang X, Yang Z, Widmalm G. Structural analysis of the exopolysaccharide produced by Streptococcus thermophilus ST1 solely by NMR spectroscopy. J Biomol NMR. 2010, 47(2):125 – 34. doi: 10.1007/s10858-010-9413-0.
25. Jamróz MK, Paradowska K, Zawada K, Makarova K, Kaźmierski S, Wawer I. $^{1}H$ and $^{13}C$ NMR-based sugar profiling with chemometric analysis and antioxidant activity of herbhoneys and honeys. J Sci Food Agric. 2014, 94(2):246 – 55. doi: 10.1002/jsfa.6241.
26. Wang Z, Zhang M, Hao L, Jiao X, Wu C. Two novel polysaccharides from Huangshui: Purification, structure, and bioactivities. Int J Biol Macromol. 2024, 267(Pt 1):131396. doi: 10.1016/j.ijbiomac.2024.131396.
27. Zhang M, Jagdmann GE Jr, Van Zandt M, Sheeler R, Beckett P, Schroeter H. Chemical synthesis and characterization of epicatechin glucuronides and sulfates: bioanalytical standards for epicatechin metabolite identification. J Nat Prod. 2013, 76(2):157 – 69. doi: 10.1021/np300568m.
28. Yuan S, Wang J, Li X, Zhu X, Zhang Z, Li D. Study on the structure, antioxidant activity and degradation pattern of polysaccharides isolated from lotus seedpod. Carbohydr Polym. 2023, 316:121065. doi: 10.1016/j.carbpol.2023.121065.

29. Tada R, Harada T, Nagi-Miura N, Adachi Y, Nakajima M, Yadomae T, Ohno N. NMR characterization of the structure of a beta-(1–>3)-D-glucan isolate from cultured fruit bodies of Sparassis crispa. Carbohydr Res. 2007, 342(17):2611-8. doi: 10.1016/j.carres.2007.08.016.
30. Zhang L, Li X, Xu X, Zeng F. Correlation between antitumor activity, molecular weight, and conformation of lentinan. Carbohydr Res. 2005, 340(8):1515-21. doi: 10.1016/j.carres.2005.02.032.
31. Ye L, Zhang J, Zhou K, Yang Y, Zhou S, Jia W, Hao R, Pan Y. Purification, NMR study and immunostimulating property of a fucogalactan from the fruiting bodies of Ganoderma lucidum. Planta Med. 2008, 74(14):1730-4. doi: 10.1055/s-2008-1081354.
32. Liu Y, Zhang J, Tang Q, Yang Y, Guo Q, Wang Q, Wu D, Cui SW. Physicochemical characterization of a high molecular weight bioactive β-D-glucan from the fruiting bodies of Ganoderma lucidum. Carbohydr Polym. 2014, 101:968 – 74. doi: 10.1016/j.carbpol.2013.10.024.
33. Mantovani A, Biswas SK, Galdiero MR, Sica A, Locati M. Macrophage plasticity and polarization in tissue repair and remodelling. J Pathol. 2013, 229(2):176 – 85. doi: 10.1002/path.4133.
34. Cendrowicz E, Sas Z, Bremer E, Rygiel TP. The Role of Macrophages in Cancer Development and Therapy. Cancers (Basel). 2021, 13(8):1946. doi: 10.3390/cancers13081946.
35. Iyer SS, Cheng G. Role of interleukin 10 transcriptional regulation in inflammation and autoimmune disease. Crit Rev Immunol. 2012 ;32(1):23–63. doi: 10.1615/critrevimmunol.v32.i1.30.
36. Yang Q, Guo N, Zhou Y, Chen J, Wei Q, Han M. The role of tumor-associated macrophages (TAMs) in tumor progression and relevant advance in targeted therapy. Acta Pharm Sin B. 2020, 10(11):2156–2170. doi: 10.1016/j.apsb.2020.04.004.
37. Nikaein N, Tuerxun K, Cedersund G, Eklund D, Kruse R, Särndahl E, Nånberg E, Thonig A, Repsilber D, Persson A, Nyman E; X-HiDE Consortium. Mathematical models disentangle the role of IL-10 feedbacks in human monocytes upon proinflammatory activation. J Biol Chem. 2023, 299(10):105205. doi: 10.1016/j.jbc.2023.105205.
38. Cai Y, Si Z, Jiang Y, Ye M, Wang F, Yang X, Yu J, Gao X, Liu W. Structure-activity relationship of low molecular weight Astragalus membranaceus polysaccharides produced by Bacteroides. Carbohydr Polym. 2023, 316:121036. doi: 10.1016/j.carbpol.2023.121036.
39. Liu Y, Zhang J, Tang Q, Yang Y, Guo Q, Wang Q, Wu D, Cui SW. Physicochemical characterization of a high molecular weight bioactive β-D-glucan from the fruiting bodies of Ganoderma lucidum. Carbohydr Polym. 2014, 101:968 – 74. doi: 10.1016/j.carbpol.2013.10.024.

# Figures

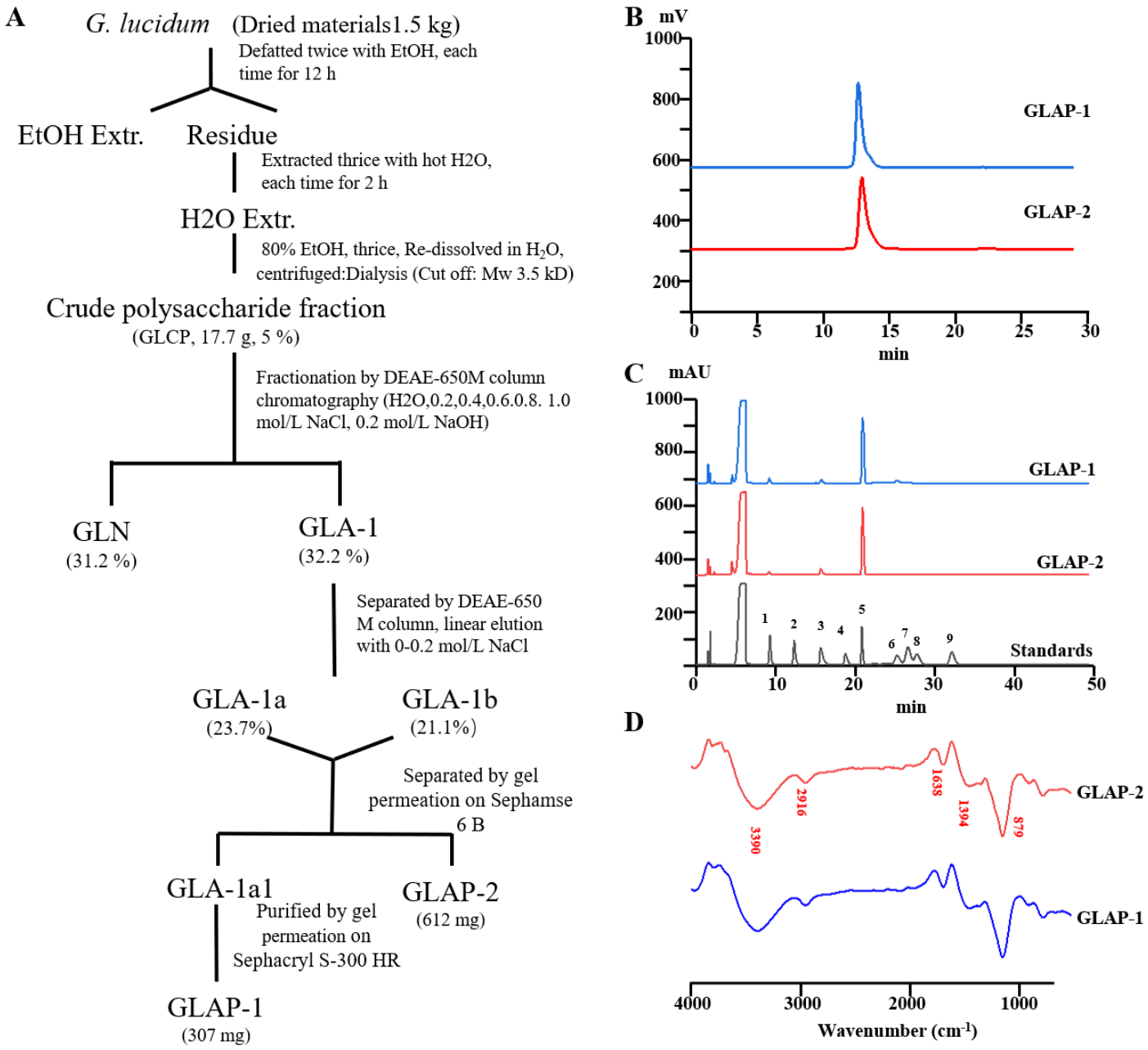
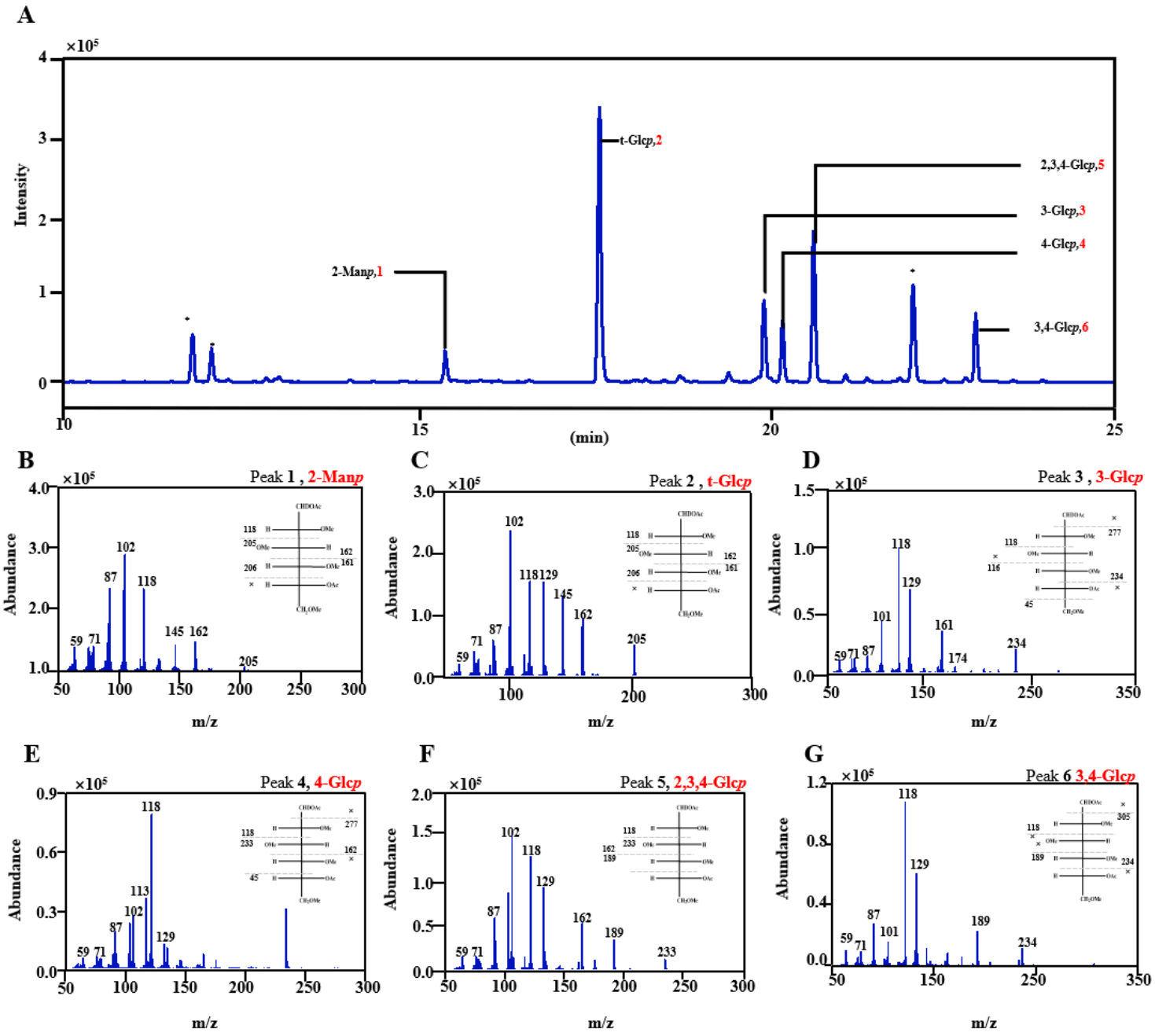



**Figure 1**

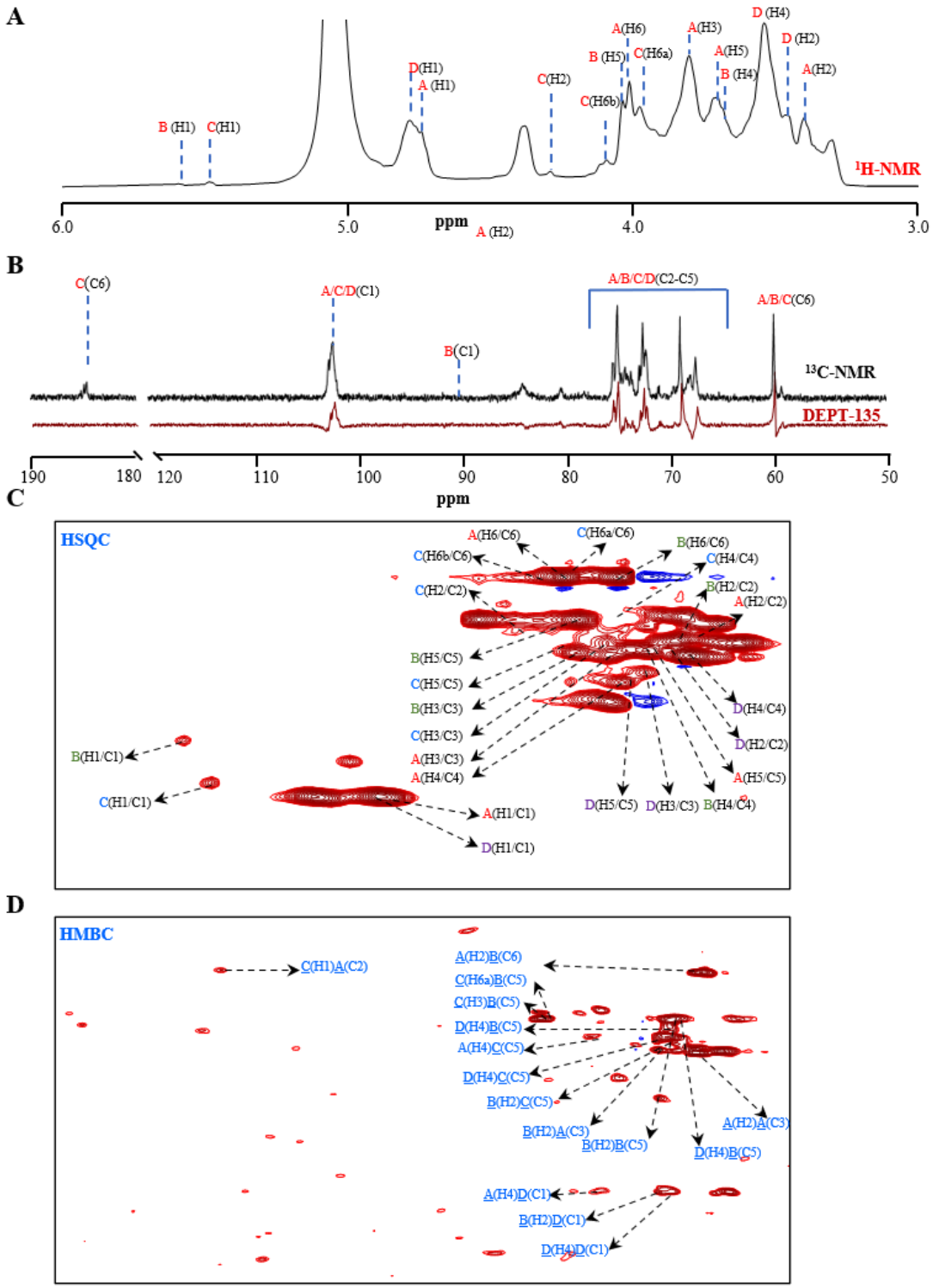
Extraction, Isolation, Purification, Physicochemical Properties and Structural Characteristics of *Ganoderma lucidum* Polysaccharides:(A) The figure for the isolation of polysaccharides from *Ganoderma lucidum ;* (B) Molecular weight of polysaccharide; (C) monosaccharide composition ; (D) FT-IR spectrum of polysaccharide

*3.2. Structural characterization of GLAP-2*




## Figure 2

Methylation analysis of GLAP-2 (A) Methylation analysis chromatogram of GLAP-2 via GC–MS. The symbol (*) denotes a non PMAA peak; (B) EI-MS spectra of peak 1. Peak number was the same as Fig. 2A.; (C) EI-MS spectra of peak 2. Peak number was the same as Fig. 2A.; (D) EI-MS spectra of peak 3. Peak number was the same as Fig. 2A.; (E) EI-MS spectra of peak 4. Peak number was the same as Fig. 2A.; (F) EI-MS spectra of peak 5. Peak number was the same as Fig. 2A.; (G) EI-MS spectra of peak 6. Peak number was the same as Fig. 2A.




## Figure 3

1D and 2D NMR spectra ofGLAP-2：A：$^{1}$H；B：$^{13}$C and DEPT 135；D：HSQC；E：HMBC

*3.3 Observation on the Effect of GLAP-2 on the Viability of RAW264.7 Cells*

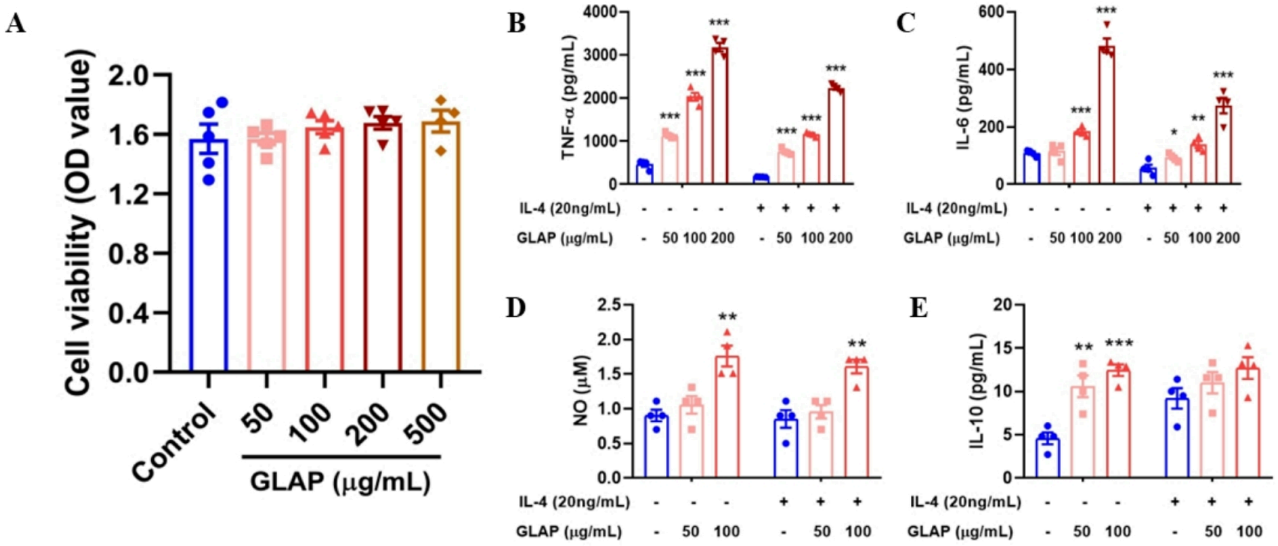



**Figure 4**

RAW264.7 Viability and M0/M2→M1 Polarization Cytokine Detection Results. (A) Effects of GLAP-2 on cell viability of RAW264.7(B) Effects of GLAP-2 on TNF-α secretion by macrophages and TAMs(C) Effects of GLAP-2 on IL-6 secretion by macrophages and TAMs

(D) Effects of GLAP-2 on NO secretion by macrophages and TAMs(E) Effects of GLAP-2 on IL-10 secretion by macrophages and TAMs

## Supplementary Files

This is a list of supplementary files associated with this preprint. Click to download.

- SupplementaryMaterials.docx